JOURNAL OF VIROLOGY, Nov. 1996, p. 8109–8116 Vol. 70, No. 11
0022-538X/96/$04.00+0

Parvovirus Minute Virus of Mice Strain i Multiplication and Pathogenesis in the Newborn Mouse Brain Are Restricted to Proliferative Areas and to Migratory Cerebellar Young Neurons

JUAN C. RAMÍREZ,[1] ALFONSO FAIRÉN,[2]† AND JOSÉ M. ALMENDRAL[1]*

Centro de Biología Molecular "Severo Ochoa" (Consejo Superior de Investigaciones Científicas-Universidad Autónoma de Madrid), Cantoblanco, 28049 Madrid,[1] and Instituto Cajal (Consejo Superior de Investigaciones Científicas), 28002 Madrid,[2] Spain

Received 26 April 1996/Accepted 24 July 1996

Newborn BALB/c mice intranasally inoculated at birth with a lethal dose of the immunosuppressive strain of the parvovirus minute virus of mice (MVMi) developed motor disabilities and intention tremors with a high incidence by the day 6 postinfection (dpi). These neurological syndromes paralleled the synthesis of virus intermediate DNA replicative forms and yield of infectious particles in the brain, with kinetics that peaked by this time. The preferred virus replicative sites in the brain were established early in the infection (2 dpi) and at the onset of clinical symptoms (6 dpi) and were compared with major regions of cellular proliferative activity found after intraperitoneal injection of bromodeoxyuridine 24 h before encephalons were subjected to immunohistochemistry detection. At 2 dpi, viral capsid antigen was located in the laterodorsal thalamic and the pontine nuclei but not in the extensive proliferative regions of the mouse brain at this postnatal day. At 6 dpi, however, the neurotropism of the MVMi was highlighted by its ability to target the subventricular zone of the ventricles, the subependymal zone of the olfactory bulb, and the dentate gyrus of the hippocampus, which are the three main germinal centers of the cerebrum in mouse postbirth neurogenesis. Unexpectedly, in the cerebellum, the MVMi capsid antigen was confined exclusively to cells that have undergone mitosis and have migrated to the internal granular layer (IGL) and not to the proliferative external granular layer (EGL), which was stained with antiproliferative cell nuclear antigen antibody and is the main target in other parvovirus infections. This result implies temporal or differentiation coupling between MVMi cycle and neuroblast morphogenesis, since proliferative granules of the EGL should primarily be infected but must migrate in a virus carrier state into the IGL in order to express the capsid proteins. During migration, many cells undergo destruction, accounting for the marked hypocellularity specifically found in the IGL and the irregular alignment of Purkinje cell bodies, both consistent histopathological hallmarks of animals developing cerebellar symptoms. We conclude that MVMi impairs postmitotic neuronal migration occurring in the first postnatal week, when, through the natural respiratory route of infection, the virus titer peaks in the encephalon. The results illustrate the intimate connection between MVMi neuropathogenesis and mouse brain morphogenetic stage, underscoring the potential of parvoviruses as markers of host developmental programs.

The genus *Parvovirus* of the family *Parvoviridae* includes a large group of nondefective small viruses containing a linear single-stranded DNA genome with a nonenveloped 25-nm-diameter icosahedral capsid (46). A general feature of parvovirus multiplication is the requirement for functions expressed during the S phase of the cell cycle (2, 49, 51). This explains why a common characteristic in the pathogenesis of these viruses is the infection of mitotically active cells and why clinical courses are more severe in developing hosts, in which many tissues are undergoing proliferation. Thus, parvoviruses are primarily teratogenic agents causing fetal and neonatal abnormalities, osteolytic syndromes, dwarfism, abortion, and malformations, although in adults they may attack tissues such as intestinal epithelium and hemopoietic system that undergo proliferation throughout life (45, 48). Parvovirus tropism is also constrained by factors expressed at certain differentiation stages (33, 47, 50), such as the receptor for the human B19 parvovirus expressed in erythroid cells (4), which accounts for the specifity of the hemopoietic disorders caused by this virus (53, 55).

Among the variety of parvovirus-caused diseases, the clinical manifestations accompanying cerebellar damage are among the most characteristic because of the essential role that this part of the central nervous system (CNS) plays in limb movement and motor control and the nonrepairability of the lesions, which leads to long-term behavioral sequelae. In mammals, an intense proliferative activity of cortical neurons at the perinatal or early postnatal period is found in the developing cerebellum (10). Precursors of granule cell neurons proliferate in the external granular layer (EGL) at a high rate, and then the soma of postmitotic daughter cells migrates inward through the molecular layer (ML) along the radial Bergmann glial fibers, extending a T-shaped axon. Postmigratory cells settle in the internal granular layer (IGL) deep in the Purkinje cell layer (PCL) and extend short dendrites (see, for example, references 1, 8, 35, and 39). The knowledge of the structure and histogenesis of the cerebellar cortex (40) provides the anatomical basis for understanding motor syndromes associated with parvovirus infections. Hence, early studies on natural infections of

* Corresponding author. Mailing address: Centro de Biología Molecular "Severo Ochoa" (CSIC-UAM), Universidad Autónoma de Madrid, Cantoblanco, 28049 Madrid, Spain. Phone: 34-1-3978048. Fax: 34-1-3978087. Electronic mail address: JMAlmendral@mvax.cbm.uam.es.

† Present address: Instituto de Neurociencias (Universidad de Alicante-Consejo Superior de Investigaciones Científicas), Campus de San Juan, 03350 San Juan de Alicante, Spain.

newborn cats with the feline panleukopenia virus (FPV) led to the association of this virus with ataxia (17), the clinical consequence of viral replication in the dividing cells of the EGL and in scattered cells of the ML and PCL (7). The infection produced lysis of the affected cell population and cerebellar hypoplasia in the kittens (17, 48).

Neurological manifestations can also be induced in experimental infections with rodent parvoviruses (reviewed in references 23 and 30) and particularly following rat virus (RV) inoculation in several hosts. Chronic ataxia with hypoplasia of the EGL could be reproduced by intracraneal inoculation of RV in newborn hamsters (18); severe granuloprival cerebellar hypoplasia occurred in newborn and suckling rats inoculated by different routes (11, 15, 20), while a lesser depletion of outer germinal cells of the cerebellum was found in cats and mice (19, 23). Hemorrhagic encephalopathy and necrotizing vasculitis, the two characteristic lesions of the CNS vascular bed, were found only in RV infections of the natural host (29). But it is poorly documented whether this or another parvovirus can replicate in CNS neural cells outside the cerebellum. More limited CNS studies have been conducted with the minute virus of mice (MVM), a common parvovirus pathogen of mouse colonies (52). The cerebellum was unaffected in transplacental infections of pregnant mice (22), and the virus induced moderate lesions in the cerebellar EGL after intracraneal and intraperitoneal inoculations of mice at birth (21). However, it is unclear whether MVM has a neuropathogenic potential in mice via more natural routes of infection.

The pathogenicity of the several mouse parvovirus isolates in infections via the more natural oronasal route has been addressed only in recent years. The prototype strain of MVM (MVMp), which infects fibroblastic cells (6), remained confined to the oropharynx of newborn mice, and the infection remained asymptomatic (24). Mouse parvovirus 1, isolated from a mouse $CD8^+$ T-cell clone (31), replicates in the intestine and lungs but does not provoke any clinical signs in orally inoculated young adult BALB/c mice (16). The immunosuppressive strain MVMi (3), which interferes with a number of T-cell functions (9) and suppresses the clonogenic capacity of different hemopoietic precursors in vitro (43), demonstrated a higher pathogenicity in oronasal infections of newborn mice. At a low dose, MVMi spread to many organs and induced a runting syndrome (24), while at a high dose, it caused a lethal infection in some inbred strains of mice, with renal papillary hemorrhage and involution of hepatic erythropoietic foci (5), as well as myeloid depression in the bone marrow and spleen (42). Despite the virulence of MVMi for neonatal mice, no CNS pathology has been found in MVMi infections.

In our latest studies on MVMi infection of susceptible newborn BALB/c mice (42), we observed neurological symptoms consistently arising in the inoculated animals. These findings suggested an inherent capacity of MVMi to target the CNS from the natural oronasal route of infection and thus to possess a clinically relevant neuropathogenic potential previously unrecognized for this virus. This issue prompted us to undertake the characterization of MVMi neurotropism with regard to CNS viral invasion, the sites of virus multiplication, and their spatial correlation with neuroblast proliferation, as well as the anatomical alterations caused by MVMi infection in the developing newborn mouse brain.

MATERIALS AND METHODS

Cell lines and virus. The EL-4 mouse C57BL T-cell lymphoma line and NB324K human simian virus 40-transformed newborn kidney cells were cultured in Dulbecco modified Eagle medium supplemented with 5% heat-inactivated fetal calf serum. MVMi was generously provided by B. Hirt (Epalinges, Switzerland) and grown by a minimal number of passages. Infectious virus was quantified by plaque assay on NB324K monolayers. Viral stocks were obtained by infection at low multiplicity of infection of EL-4 lymphoma cultures from which it was originally isolated (3). For inoculation of the mice, and in order to minimize the immune recognition of input particles, only virus purified by CsCl gradients (43) devoid of empty capsids was used.

Mice and viral inoculations. The mouse C57BL/6 and BALB/c inbred strains were originally purchased from the Jackson Laboratory (Bar Harbor, Maine) and bred in our animal facility under standard conditions. Pregnant mice 8 to 12 weeks of age were individually housed in environmental isolated cabinets (IFFA-CREDO) to prevent contamination during analysis of the offspring. Dams were routinely proved to be seronegative to MVM capsid antigens by an enzyme-linked immunosorbent assay as described previously (42).

Because the susceptibility to lethal infection of the sensitive mouse strains relies greatly on the age of newborn mice, dams were observed twice daily for parturition and infected as soon after birth as possible and never later than 24 h postbirth. To improve homogeneity, infected as well as control litters were normalized to seven animals. Mice were inoculated intranasally by carefully placing over the animal nostrils 5 μl of viral suspension containing 10^6 PFU in phosphate-buffered saline (PBS). Control animals were inoculated with 5 μl of PBS. Complete inhalation of virus inocula was carried out. When indicated, mice were injected intraperitoneally with bromodeoxyuridine (BrdU) at a dose of 20 mg/kg of body weight to label brain cells in S phase.

Analysis of virus multiplication in the CNS. Neonatal mice were euthanized at various times under an ether atmosphere, and the brains were aseptically removed. The portion caudal with respect to the corpora quadrigemina, containing the cerebellum and the brain stem, was separated from the forebrain and midbrain through a dorsoventral section. For practical purposes, the rostral portion is referred to as cerebrum and the caudal portion is referred to as cerebellum. Cerebra and cerebella of infected mice were dissected aseptically, weighed, and disrupted in 10% (wt/vol) PBS (0.1 M $NaPO_4$ [pH 7.2], 0.875 g of NaCl per liter), using an ULTRA-TURRAX T25 homogenizer. The homogenate was frozen and thawed twice and centrifuged to remove debris, and the infectious virus titer in the supernatant was determined by plaque assay. Under these conditions, the limit of the assay was 2.5 PFU/g of tissue.

To determine viral DNA in the brain, homogenates were quickly adjusted to 50 mM Tris (pH 8)–10 mM EDTA–1% sodium dodecyl sulfate and digested with 100 μg of proteinase K (Merck) per ml for 2 h at 37°C. Digested tissues were processed for low-molecular-weight DNA enrichment by a modified Hirt method (32), supplementing with 20 μg of carrier tRNA (Boehringer) to ensure quantitative recoveries. DNA was subjected to electrophoresis on a 1.0% agarose gel and alkali blotted to nylon Hybond-N^+ membranes (Amersham). The membranes were baked to affix the DNA, prehybridized, probed with a ^{32}P-labeled full-length cloned MVM DNA (specific activity, 10^9 cpm/μg), and washed as previously described (38). The filters were dried and exposed to X-ray film for the indicated period of time.

Histological preparations. For brain fixation, deeply anesthetized mice were perfused transcardially for 20 min with paraformaldehyde fixative (4% paraformaldehyde, 0.1 M $NaPO_4$ [pH 7.2], 0.875 g of NaCl per liter). Alternatively, whole organs were rapidly and aseptically removed from euthanized mice, rinsed in PBS, and maintained in the same buffer for no longer than 1 week before processing for histochemistry.

Tissues were embedded in melted 4% agar (Merck), cooled, and cut into 100-μm-sections in coronal or sagittal orientation on a Vibratome under 0.1 M phosphate buffer (pH 7.2). The free-floating sections were processed for immunohistochemistry in glass scintillation vials the same day. Alternatively, fixed organs were dehydrated through increased graded alcohol, embedded in paraffin, sliced in 14-μm-thick sections, and stained in standard Harris hematoxylin and eosin for histopathology examination.

Immunohistochemistry. An immunoperoxidase procedure was chosen for detection of primary bound antibodies. Endogenous peroxidase was inactivated by pretreatment of sections with 3% (vol/vol) H_2O_2 and 10% (vol/vol) methanol in 0.1 M phosphate buffer (pH 7.2) for 15 min. Sections were treated for 30 min in PBS containing 0.25% (wt/vol) gelatin–0.1 M lysine, rinsed twice in PBS, and incubated with the corresponding primary antibody.

Viral structural proteins were detected with a polyclonal hyperimmune rabbit anti-MVM capsid antiserum that stains denatured structural MVM proteins (41) and also neutralizes infectivity (43). The antiserum was enriched in immunoglobulin G by affinity purification through a protein A-Sepharose column and used at 1/100 dilution in PBS-gelatin. As the secondary antibody, a biotinylated goat anti-rabbit (Jackson Laboratory) at 1/100 dilution was used, and the signal was amplified with avidin-biotinylated horseradish peroxidase complex (Vectastain Elite ABC kit; Vector Laboratories) as instructed by the manufacturer. Bound peroxidase was revealed with 0.05% (wt/vol) diaminobenzidine tetrahydrochloride and 0.01% (vol/vol) H_2O_2 in PBS. Method specificity was controlled by incubating sections from infected mice with rabbit preimmune sera and secondary antibody.

Incorporated BrdU on brain cell DNA was detected by using an undiluted mouse monoclonal antibody (Boehringer) reactive to the BrdU ligand and processed for immunoperoxidase as described above, with addition of a step of denaturation of double-stranded DNA with 2 N HCl in PBS for 30 min and further neutralization with 0.1 M NaB_4O_7 after inactivation of endogenous

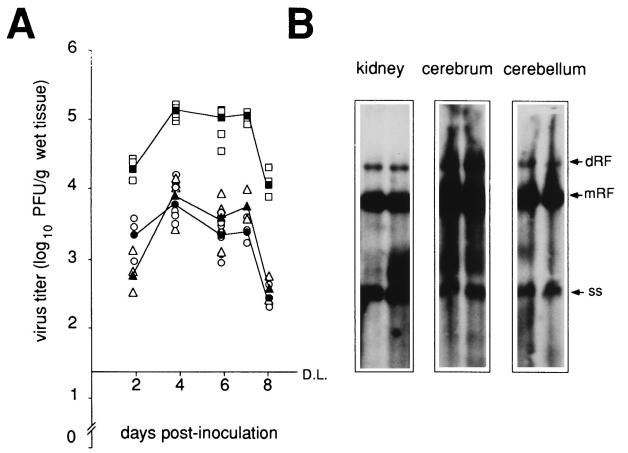

FIG. 1. Time course of MVMi multiplication in the brains and kidneys of intranasally infected newborn mice. (A) Infectious virus production. The virus titers present in the cerebrum (circles), cerebellum (triangles), and kidney (squares) at the indicated days postinoculation are shown. Mice were sampled from at least two normalized litters. Each point is the average value of two independent titrations of each sample. Filled symbols represent the mean value for each day and organ. D.L., detection limit of the assay. (B) Analysis by Southern blotting of MVMi DNA replication in the indicated organs of two mice at day 6 postinoculation. Low-molecular-weight DNA isolated from 5 mg of organ was loaded per slot. The positions of the dimeric and monomeric replicative intermediates (dRF and mRF) and genomic (single-stranded [ss]) DNA forms were determined from markers run on the same gel (42) and are indicated at the right. The exposure time for brain samples (96 h) was 10 times that for kidney samples.

peroxidase. Neuroblasts containing proliferating cell nuclear antigen (PCNA) were detected by incubation with mouse monoclonal anti-PCNA immunoglobulin (Boehringer). Sections were air dried on gelatinized slides and mounted with DPX (BDH).

RESULTS

Clinical disease and course of MVMi infection in the CNS of oronasally inoculated newborn mice. BALB/c mice inoculated intranasally within the first 24 h of life with a lethal dose of 10^6 PFU of purified MVMi developed neurological symptoms commonly from day 4 postinfection. The behavioral symptoms exhibited by the mice included sluggishness, intention tremors, and ataxic gait, which are motor disabilities characteristic of cerebellar dysfunction. We have observed these symptoms in 70% of the infected animals from a total of six litters normalized to seven mice each. These neurological syndromes lasted until the death of the animals, and in some cases (around 8%) the animals showed aggravated symptoms together with dwarfism and a darker skin. In the whole infected population, the mortality was slightly higher than previously reported (42); the average day of death was day 8 ± 1.5 postinfection, and all of the inoculated mice were dead by 12 days postinfection (dpi).

To initially study whether the neurological symptoms could be accounted for by an ability of MVMi to access and multiply in the mouse CNS, we determined the extent of infectious virus presence in the caudal and rostral parts of the brains (cerebellum and cerebrum, respectively) of the infected mice. The kidney was taken from each of the same animals as a reference because of the previously described high MVMi multiplication in this organ (5). Infectious virus was detectable in the brain as early as 2 dpi, with a titer fivefold lower in the cerebellum than in the cerebrum (Fig. 1). At 4 dpi, infectivity titers in the brain reached a maximum, remained essentially stable from 4 to 7 dpi, and then declined by 8 dpi. These kinetics paralleled those found for the kidney at values 20- to 50-fold higher (Fig. 1A) and the results found for other organs in similar MVMi infections of newborn mice (5, 42).

The infectious particles isolated from the brain homogenates may correspond to a viremia in the blood vessels of the CNS and not to virus produced in neural tissue. To determine whether MVMi actually replicates in the brain, we isolated low-molecular-weight DNA from the cerebella and cerebra of the animals during week 1 postinfection and analyzed by blot hybridization the synthesis of viral DNA. Figure 1B shows one analysis of this type performed for two animals at 6 dpi. As shown in Fig. 1B, MVMi could synthesize DNA in the mouse brain, as judged by the accumulation of monomeric and dimeric intermediate replicative DNA forms. Moreover, single-stranded genomic forms corresponding to encapsidated molecules were also reliably detected, an indication that viral maturation also takes place in the brain.

The sites of parvovirus MVMi multiplication within the developing mouse brain. Even with the low levels of infectious virus and DNA replication found in the brain, the limited areas where neural cells undergo proliferation after birth may limit MVMi multiplication to specific CNS centers, where a local accumulation of virus antigens could cause extensive cellular damage. Thus, we explored MVMi neuropathogenic potential by determining the CNS sites where MVMi multiplies and its relationship with cellular proliferation at two stages of the infection: (i) 2 days after intranasal inoculation, when infectious virus in the brain was already detectable, and (ii) at the peak of virus multiplication at 6 dpi, when neurological symptoms were evident in many inoculated animals.

For studying virus multiplication and cell proliferation at early times of the infection, mice oronasally infected at birth were injected with a single dose of BrdU 24 h postinfection and sacrificed 24 h later. Brains were removed, and serial parasagittal sections were stained with specific antibodies for MVMi capsid and BrdU. Selected regions representative of the entire analysis are shown in Fig. 2. The preferential areas of MVMi antigen expression were found in the laterodorsal thalamic nuclei and in the pontine nuclei (Fig. 2d and f), even though relatively few proliferative cells were found in these regions (Fig. 2c and e). In contrast, regions with a high density of cells undergoing proliferation, such as the EGL of the cerebellum (not shown) or the lining of the lateral ventricle and the hippocampal formation (Fig. 2a), were consistently negative for viral antigens (Fig. 2b). Therefore, proliferative structures are not preferentially targeted by MVMi at early time of CNS infection. This result suggests a selective route of invasion by MVMi into the brain, as well as a restricted traffic of infectious particles to areas where proliferative cells accumulate.

For the analysis at 6 dpi, BrdU was administered at 5 dpi and brain samples were processed similarly. At the height of the infection at 6 dpi, by the time when most animals became clinically symptomatic, a completely different pattern of viral capsid antigen distribution was found in the mouse brain. Besides many blood vessels with positive staining of endothelial cells across the brain parenchyma (Fig. 3e), major areas of positively stained cells included the following: in the hippocampal formation, the viral antigens localized preferentially in cells of the dentate gyrus (Fig. 3a) and not in the structures that compose the Ammon's horn; the olfactory bulb also shows abundant cells stained for viral antigens in the subventricular zone as well as scattered positive cells in the surrounding granular cell layer (Fig. 3b); a third main area of viral replication was the lateral ventricle, the positive cells being located in the subventricular zone (Fig. 3d). All of these structures are germinal centers in mouse postbirth neurogenesis on postnatal day 6 (P6) (reference 14 and references therein) and as such

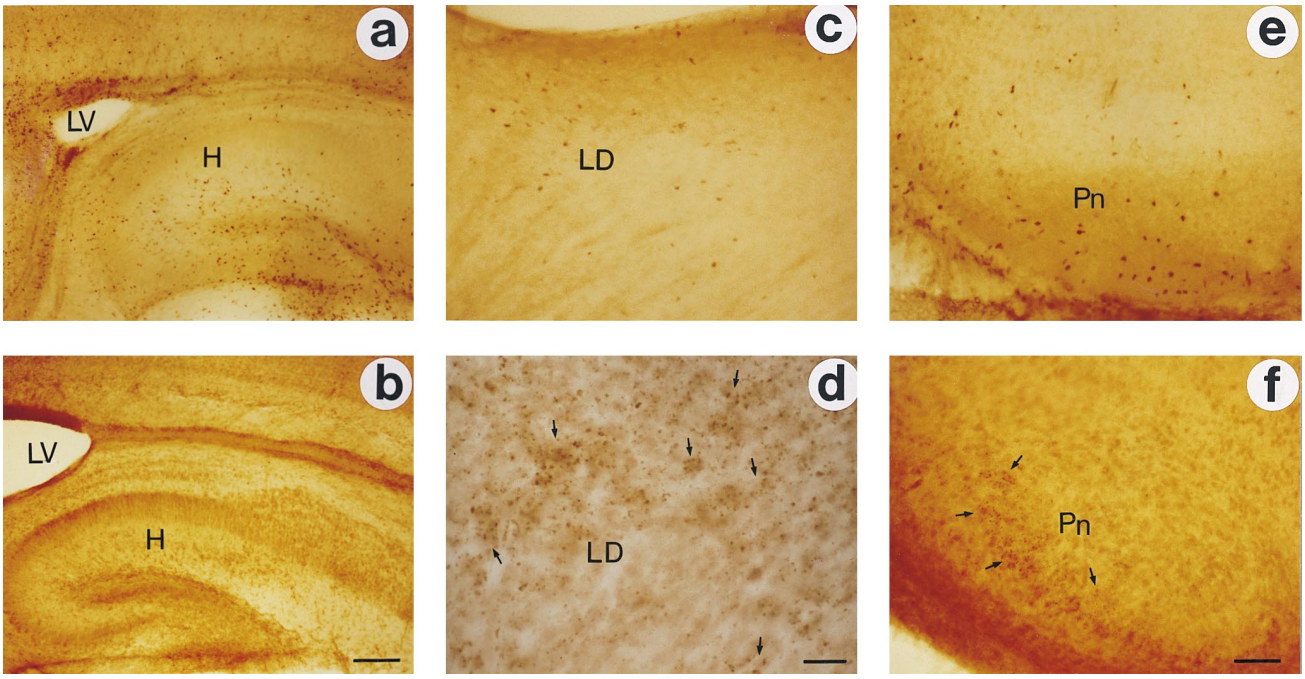

FIG. 2. Localization of MVMi antigens in the mouse brain at early stages of infection in relation to the regional proliferative activity of neuroblasts. Mice infected with MVMi at birth were in vivo labeled 24 h later with a single dose of BrdU. At 2 days of age, the animals were sacrificed and Vibratome serial slices (100-μm thickness) were probed for virus capsid antigens (b, d, and f) or BrdU (a, c, and e). Areas with virus-positive cells are marked by arrows. Scale bars indicate 100 μm for the hippocampal region (a and b), 50 μm for the thalamus (c and d), and 50 μm for the pons (e and f). Abbreviations: H, hippocampus; LV, lateral ventricle; LD, laterodorsal thalamic nuclei; Pn, pontine nuclei.

were labeled by BrdU administered at 5 dpi and developed 24 h later in sections contiguous to those where the viral antigens were found (not shown). Outside the cerebrum, the major concentration of positive cells was found in the cerebellum, but surprisingly, the stained cells were confined to the outer half of the IGL all along the folia (Fig. 3c) and not to the EGL, where BrdU labeling, denoting proliferative activity, accumulated (see below).

Expression of MVMi capsid proteins along young neurons migrating between cerebellar layers. The fact that MVMi antigen expression was detected in the IGL rather than in the postnatal proliferatively active EGL contradicted the known requirement of cell proliferation for parvovirus multiplication. Therefore, we undertook a new set of experiments to study MVMi multiplication in the context of the pattern of division and migration that governs morphogenesis of the cerebellar layers on P6. For this purpose, BrdU labeling to stain proliferative cells was administered in the infected mice either 24 h (as described above) or 48 h before analysis at 6 dpi. In the 24-h BrdU labeling (Fig. 4, left), the entire thickness of the EGL was stained, and some labeled cells were also seen in the white matter. When BrdU labeling was performed 48 h before analysis (Fig. 4, right), most labeled cells had migrated inward to the IGL, and only scattered cells remained in the EGL. However, a parallel staining for PCNA, a universal marker of cellular DNA synthesis (34), indicated that cells traversing the S phase of the cell cycle remained restricted to the EGL (Fig. 4, right), and so cells settled in the IGL were not proliferative by the time of analysis. Therefore, there is apparently no self-renewing of proliferative cells in the EGL, since most cells undergoing DNA synthesis are committed to migrate through the ML. Significantly, throughout these experiments we found again the virus-positive cells confined to the IGL irrespective of the timing of BrdU administration (results of 24-h labeling are shown in Fig. 4). These data demonstrate that the productively infected cerebellar neuroblasts must have undergone DNA synthesis in the EGL as well as migration inward to the IGL. Both events are required for MVMi capsid protein synthesis to occur.

Histopathological findings in MVMi-infected newborn mouse brain. The neuropathological symptoms found in the animals may result from a local injury in those brain regions where MVMi multiplication was confined. To explore the histopathological bases of this disease, brains from P6 mice showing impaired motor coordination were fixed, embedded in paraffin, and thin sectioned, and the slides were subjected to microscopic examination for comparison with uninfected brains of age-matched mice. Neither hemorrhagic encephalopathy nor aplasia or gross malformations were observed in the whole encephalon of the infected mice compared with controls, although a small reduction in the overall size was often noted. At high magnification, however, some anatomical alterations were found in the infected P6 cerebellar cortex (Fig. 5). The major change in cell structure was a hypoplastic IGL, with a much lower cell density and width than in the control. This feature was consistently accompanied by a slightly narrower ML and a PCL with uneven cellular alignment and less apparent cell bodies (Fig. 5, bottom). Nevertheless, no changes were found in the cellular composition of the EGL, since the thickness and the number of rows of granule cells (approximately eight in the first postnatal week of the mouse [10]) were comparable in control mice and mice showing clinical signs. Altogether, these findings demonstrate that MVMi impairs cerebellum morphogenesis by infecting and lysing migratory granule cells. These cerebellar lesions may account for the behavioral and motor coordination alterations found in the infected mice.

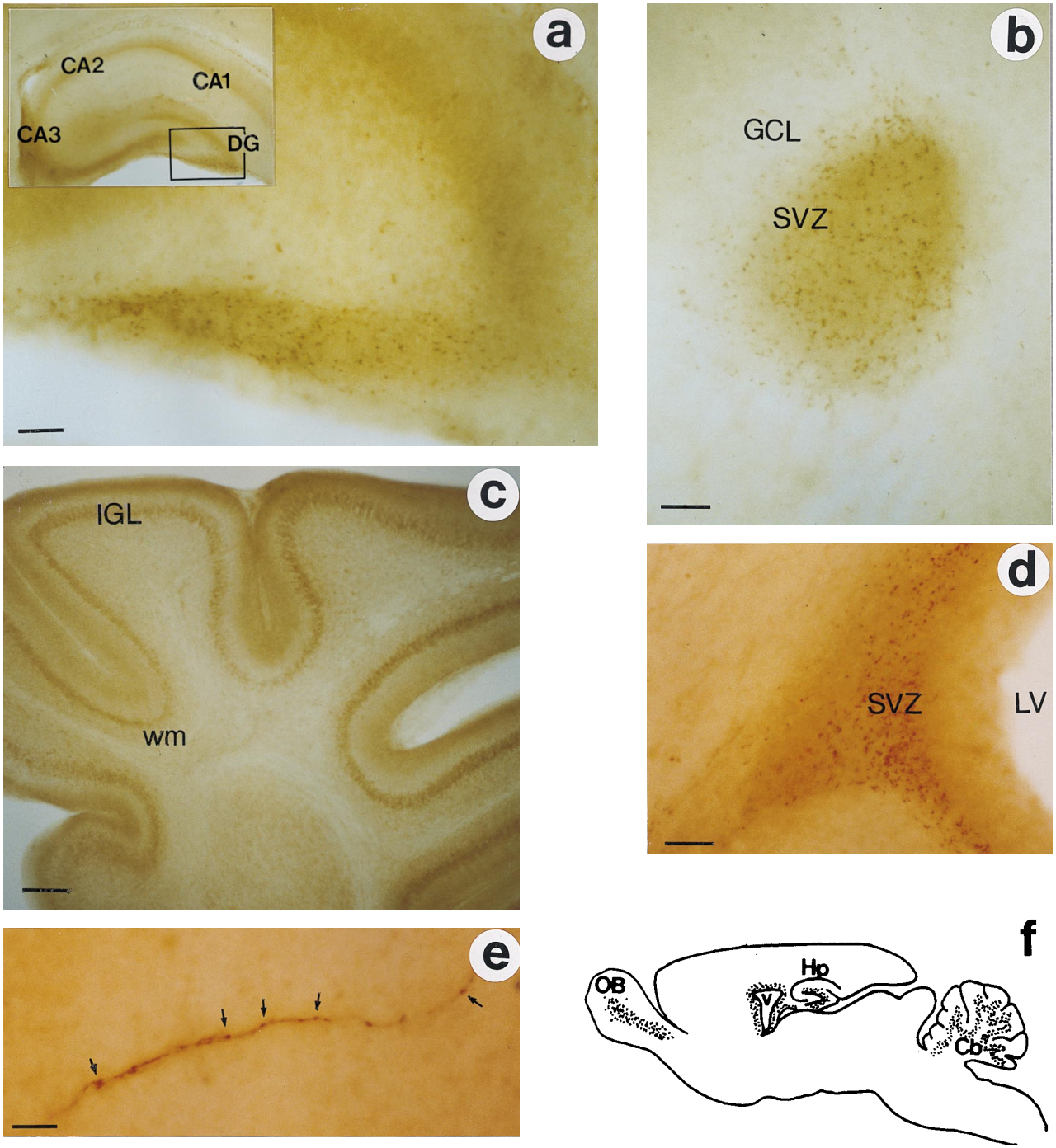

FIG. 3. Pattern of MVMi infection in the brains of newborn mice at 6 dpi. Bright-field photomicrographs show immunoperoxidase staining of MVMi-infected cells in the brains of mice at 6 dpi. Vibratome sections (100 μm thick) were used to detect viral capsid antigens. (a) Hippocampus with a magnification of the dentate gyrus; (b) olfactory bulb; (c) cerebellum; (d) lateral ventricle; (e) blood vessel with stain of virus-positive endothelial cells (arrows); (f) sagittal schematic representation of the mouse brain depicting the CNS distribution of MVMi-positive cells by 6 dpi (shaded areas). Abbreviations: CA1, CA2, and CA3, Ammon's horn; DG, dentate gyrus; GCL, granular cell layer; IGL, internal granular layer; wm, white matter; LV, lateral ventricle; SVZ, subventricular zone; OB, olfactory bulb; V, ventricle; Hp, hippocampus; Cb, cerebellum. Scale bars: 50 μm in the coronal sections (a, b, and c); 25 μm in panel e; 100 μm in the parasagittal section (c).

DISCUSSION

We have studied the in vivo neurotropism of the parvovirus MVMi in BALB/c mice, determining the viral spread, distribution, and neuropathology in the newborn. MVMi naturally inoculated onto the oronasal cavity was able to reach and replicate in neural tissue of newborn mice and should therefore be classified as a true neurotropic virus. Via respiratory infection, MVMi entered the bloodstream and multiplied in most organs of the newborn (5, 42). The common finding of virus-positive vascular endothelial cells scattered throughout the brain parenchyma (Fig. 3) favors this route as the one followed by the virus to invade the CNS. In previous studies,

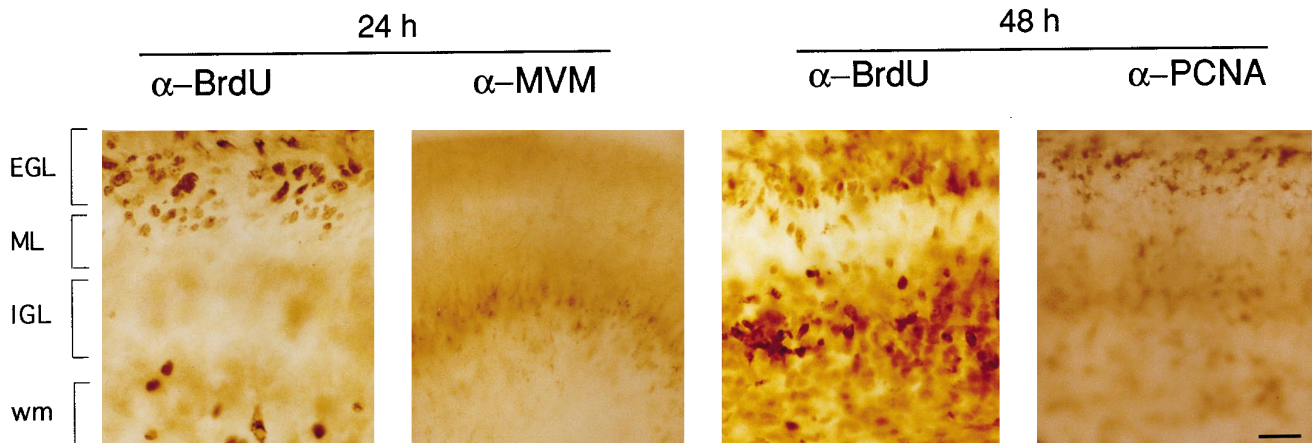

FIG. 4. Proliferation and cell migration in the cerebellar granular layers of MVMi-infected newborn mice. BALB/c mice infected at birth with MVMi were intraperitoneally injected with BrdU either 24 or 48 h before analysis at 6 dpi. Brains were removed, and serial parasagittal Vibratome sections (100 μm thick) were probed with a monoclonal antibody against BrdU (α-BrdU) or PCNA (α-PCNA) or with an antiviral capsid polyclonal antibody (α-MVM). Scale bar, 25 μm. wm, white matter.

some inbred strains of mouse were susceptible, and the animals died a few days postinoculation with histopathological findings in the kidney not seen in the resistant strains (5). In this work, the CNS is added as another vital system in which MVMi multiplies, and causing neurological motor symptoms and depopulation of the IGL of the cerebellum in susceptible BALB/c mice. Significantly, we were unable to demonstrate any of these features in resistant C57BL/6 mice (37), in agreement with the reported lack of infectious virus in the brains of mice of this strain (5). Therefore, neurotropism seems to be a relevant factor of MVMi virulence and a major determinant of the lethal outcome of the infection in susceptible strains.

In the context of parvovirus-host interactions, the common tropism of MVMi and FPV for hemopoietic and neuronal cells (7, 17, 26, 43) raises the question of whether the also hematotropic human B19 parvovirus (53, 55) may be involved in neurological damage. Evidence for an association between B19 intrauterine infections and CNS disease with potential long-term sequelae in liveborn infants has been reported (54), although the pathogenesis is unclear since B19 infection of nonerythroid cells has not been described. In this regard, it may be worth stressing that MVMi neuropathogenicity was demonstrated in mice inoculated at birth with a high virus load, that the low number of cells targeted by the virus was seen only in thick histological sections, and that these cells were restricted to specific sites giving a pattern of spatial distribution changing as development progressed.

We have focused our study on the cerebellum because of the

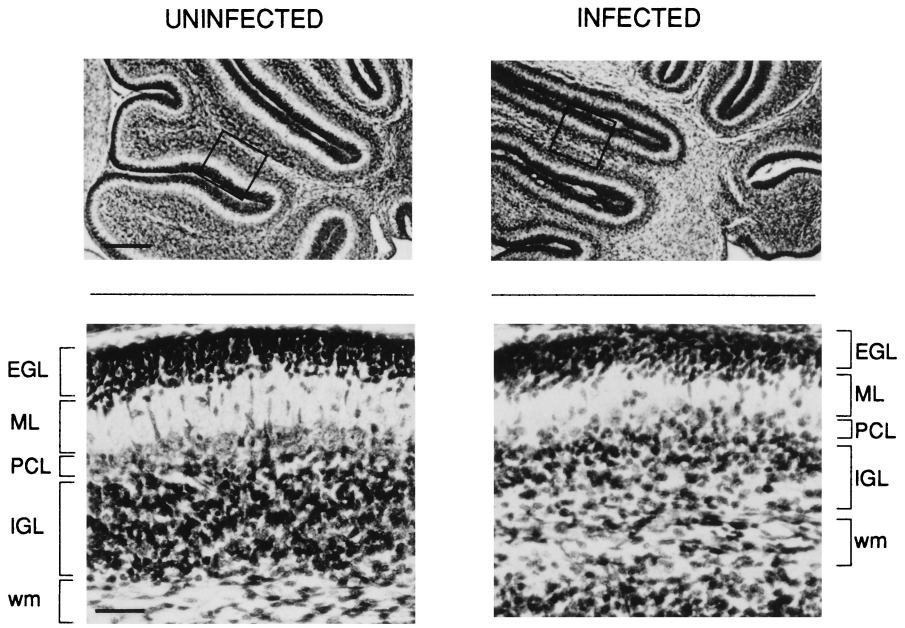

FIG. 5. Cerebellar histopathology of MVMi-infected newborn mice. Newborn mice were inoculated at birth and sacrificed at day 6 with the onset of tremors. Paraffin embedded brains were parasagitally sectioned at 14 μm and hematoxylin-eosin stained. Photomicrographs of uninfected and infected animals are shown; the squared areas in the low-power photographs are magnified at the bottom. Scale bars indicate 200 μm (upper panels) and 40 μm (lower panels). wm, white matter.

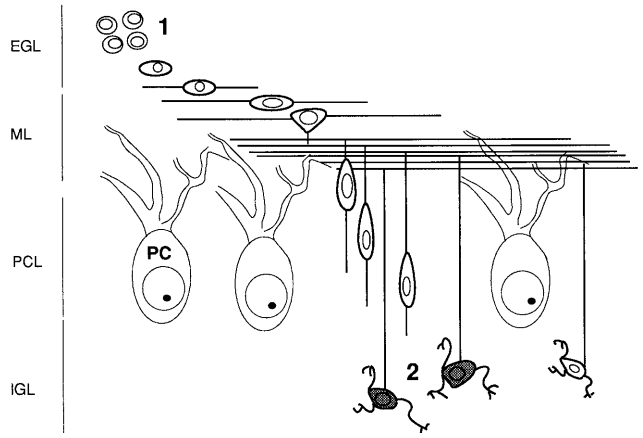

FIG. 6. MVMi capsid expression in the migratory cerebellar granule cells. The drawing shows the main features of granule cell development in the cerebellum, including proliferation in the EGL, extension of parallel fibers in the ML, and the postmitotic descending process of the cell body into the IGL with dendritic branching. The expression of MVMi capsid is localized in the differentiated neurons of the IGL (shadowed cells indicated by number 2) and not in the proliferating precursor cells of the EGL (number 1). PC, Purkinje cell. Modified from reference 40.

detailed information available on the morphogenesis of the germinal layers and the possibility to compare the effects of MVMi infection with other parvovirus infections. Unlike natural FPV infections or experimental inoculations with rodent parvoviruses in which viral multiplication occurred mainly in the EGL (17, 30), MVMi structural protein synthesis after oronasal inoculations of newborn mice was detected only in the IGL (Fig. 6). This result may be explained by the timing of CNS invasion by MVMi with respect to cerebellar histogenesis. During the first postnatal week, an intensive proliferative activity of the neuroblasts increases the width of the EGL (13), but at 2 dpi, the MVMi capsids were strictly confined to areas of the cerebrum with limited proliferative activity (Fig. 2), suggesting that at this time postinfection, the viral load in the CNS may be insufficient to reach the EGL. The titer of virus in the CNS and in other organs reached a peak by 4 to 6 dpi (Fig. 1A), when a significant migration of granule cells from the EGL to their final destination in the IGL had started (10). In fact, the BrdU label at 6 dpi remained in the EGL 24 h after injection but was in the IGL 48 h later (Fig. 4). Therefore, when the higher viral load invades the cerebellum, neuroblastic cells that undergo DNA synthesis are committed to migrate. The fact that capsids are detected only in the IGL may thus indicate a coincidence between the timing of MVMi late gene expression and the transit time of the postmitotic neurons traversing the ML toward the IGL. Alternatively, a requirement for a certain differentiation stage could underlie MVMi protein expression, if EGL neuroblasts are not susceptible to MVMi before they migrate inward. During migration, granule cells undertake a complex differentiation program that includes the cessation of DNA synthesis (10), morphological changes (40), the concurrence of multiple molecular events (35), and a pattern of gene expression (25, 56). Migratory infected neurons may synthesize MVMi capsids only at a precise step of this morphogenetic pathway, in analogy to the requirement for developmentally regulated factors proposed for in vitro MVM infections (33, 47, 50).

The different cerebellar layer where MVMi capsids localize compared with the site of multiplication of other parvoviruses is reflected in the characteristic histopathology of each infection. FPV and RV replicate in the EGL, leading to the destruction of the proliferative neuroblasts and to a global cerebellar hypoplasia in the surviving animals (17, 18). MVMi oronasal infection neither macroscopically perturbs the cerebellum anatomy nor reduces the number of cell rows of the EGL. But the IGL, where the capsid antigen was localized at 6 dpi, showed a lower cell density than in the uninfected mice and the PCL was less strictly aligned (Fig. 5), both suggesting a destruction of the postmitotic granule cells either as they move across the ML or once they have settled in the IGL. It is noteworthy that these two grades of cerebellar cortex histopathology parallel the cytoarchitecture found in mutant mice harboring different gene dosages of the autosomal recessive *weaver* mutation. This gene seems to function in the local interactions among progenitor cells required for the extension of neurites and migration (12). In the homozygous *weaver* mouse (44), the neurons die close to the sites of genesis in the EGL during the first 2 weeks after birth, leading to degeneration of the EGL and to a drastic cerebellar hypoplasia, which resembles the FPV and RV infections as previously noted (30). In the *weaver* heterozygote, the major defect is an abnormality of postmitotic granule cell migration (36), and the cerebellar phenotype in this mouse is remarkably similar to the pathological features of MVMi infection. Therefore, the MVMi-infected neuroblasts fail in their morphogenetic program at the same state at which the dose of the *weaver* gene becomes limiting in the heterozygote. In both situations, but through different mechanisms, the migratory neurons would be unable to proceed with the cellular recognitions required for promoting processes and synaptic connections (40), accounting for the thinner IGL and the loss of alignment of the PCL.

Although not addressed in this work, the death of migratory postmitotic neurons is also expected to occur in the other sites of the cerebrum that undergo postbirth proliferation and where MVMi multiplies. In the target areas of the hippocampus and of the olfactory bulb, it is likely that MVMi infection lowers cell density and impairs neuronal interactions, leading to neuroanatomical alterations. Moreover, the fact that MVMi infection mimics the above-mentioned genetic migration failure allows us to hypothesize that this parvovirus may be used as a selective ablative agent to trace patterns of proliferative activity and pathways of migration of ventricular cells (27, 28), paralleling the data shown here for the cerebellar layers.

ACKNOWLEDGMENTS

We thank G. Siegl for critical reading of the manuscript and A. Smith-Fernández and I. DeDiego for experimental assistance during the early stages of this research. The help of J. Pérez in Parafilm embedding is also gratefully acknowledged.

This work was supported by grants SAF 95-0202 from the Comisión Interministerial de Ciencia y Tecnología and PM 92-0019 from the Dirección General de Investigación Científica y Técnica, contract BMH1-CT92-0629 from the Commission of the European Communities, and an institutional grant from Fundación Ramón Areces to the Centro de Biología Molecular "Severo Ochoa."

REFERENCES

1. **Altman, J.** 1972. Postnatal development of the cerebellar cortex in the rat. III. Maturation of the components of the granular layer. J. Comp. Neurol. **145:**465–514.
2. **Berns, K. I.** 1990. Parvovirus replication. Microbiol. Rev. **54:**316–329.
3. **Bonnard, G. D., E. K. Manders, D. A. Campbell, R. B. Herberman, and M. J. Collins.** 1976. Immunosuppressive activity of a subline of the mouse EL-4 lymphoma. J. Exp. Med. **143:**187–205.
4. **Brown, K. E., S. M. Anderson, and N. S. Young.** 1993. Erythrocyte *P* antigen: cellular receptor for B19 parvovirus. Science **262:**114–117.
5. **Brownstein, D. G., A. L. Smith, R. O. Jacoby, E. A. Johnson, G. Hansen, and P. Tattersall.** 1991. Pathogenesis of infection with a virulent allotropic variant of minute virus of mice and regulation by host genotype. Lab. Invest. **65:**357–363.

6. **Crawford, L. V.** 1966. A minute virus of mice. Virology **29:**605–612.
7. **Csiza, C. K., A. de Lahunta, F. W. Sacott, and J. H. Gillespie.** 1971. Pathogenesis of feline panleukopenia virus in susceptible newborn kittens. Infect. Immun. **3:**838–846.
8. **Eccles, J. C., M. Ito, and J. Szentagothai.** 1967. The cerebellum as a neuronal machine. Springer-Verlag, New York.
9. **Engers, H. D., J. A. Louis, R. H. Zubler, and B. Hirt.** 1981. Inhibition of T-cell mediated functions by MVM(i), a parvovirus closely related to minute virus of mice. J. Immunol. **127:**2280–2285.
10. **Fujita, S.** 1967. Quantitative analysis of cell proliferation and differentiation in the cortex of the postnatal mouse cerebellum. J. Cell Biol. **32:**277–286.
11. **Gaertner, D. J., R. O. Jacoby, E. A. Johnson, F. X. Paturzo, A. L. Smith, and J. L. Brandsma.** 1993. Characterization of acute rat parvovirus infection by in situ hybridization. Virus Res. **28:**1–18.
12. **Gao, W.-Q., and M. E. Hatten.** 1993. Neuronal differentiation rescued by implantation of weaver granule cell precursors into wild-type cerebellar cortex. Science **260:**367–369.
13. **Jacobson, M.** 1991. Histogenesis of the cerebellar cortex, p. 432–441. *In* M. Jacobson (ed.), Developmental neurobiology. Plenum, New York.
14. **Jacobson, M.** 1991. Time and sequence of origin of neurons and glial cells in the central nervous system, p. 58. *In* Developmental neurobiology. Plenum, New York.
15. **Jacoby, R. O., P. N. Bhatt, D. J. Gaertner, A. L. Smith, and E. A. Johnson.** 1987. The pathogenesis of rat virus infection in infant and juvenile rats after oronasal inoculation. Arch. Virol. **95:**251–270.
16. **Jacoby, R. O., E. A. Johnson, L. Ball-Goodrich, A. L. Smith, and M. D. McKisic.** 1995. Characterization of mouse parvovirus infection by in situ hybridization. J. Virol. **69:**3915–3919.
17. **Johnson, R. H., G. Margolis, and L. Kilham.** 1967. Identity of feline ataxia virus with feline panleucopenia virus. Nature (London) **214:**175–177.
18. **Kilham, L., and G. Margolis.** 1964. Cerebellar ataxia in hamsters inoculated with rat virus. Science **143:**1047–1048.
19. **Kilham, L., and G. Margolis.** 1965. Cerebellar disease in cats induced by inoculation of rat virus. Science **148:**244–246.
20. **Kilham, L., and G. Margolis.** 1966. Spontaneous hepatitis and cerebellar hypoplasia in suckling rats due to congenital infection with rat virus. Am. J. Pathol. **49:**457–475.
21. **Kilham, L., and G. Margolis.** 1970. Pathogenicity of minute virus of mice (MVM) for rats, mice and hamsters. Proc. Soc. Exp. Biol. **133:**1447–1452.
22. **Kilham, L., and G. Margolis.** 1971. Fetal infections of hamsters, rats and mice induced with the minute virus of mice (MVM). Teratology **4:**43–62.
23. **Kilham, L., and Margolis.** 1975. Problems of human concern arising from animal models of intrauterine and neonatal infections due to viruses: a review. Prog. Med. Virol. **20:**113–179.
24. **Kimsey, P. B., H. D. Engers, B. Hirt, and V. Jongeneel.** 1986. Pathogenicity of fibroblast- and lymphocyte-specific variants of minute virus of mice. J. Virol. **59:**8–13.
25. **Kuhar, S. G., L. Feng, S. Vidan, M. E. Ross, M. E. Hatten, and N. Heintz.** 1993. Changing patterns of gene expression define four stages of cerebellar granule neuron differentiation. Development **117:**97–104.
26. **Kurtzman, G. J., L. Platanias, L. Lustig, N. Frickhofen, and N. S. Young.** 1989. Feline parvovirus propagates in cat bone marrow cultures and inhibits hematopoietic colony formation in vitro. Blood **74:**71–81.
27. **Lois, C., J. M. García-Verdugo, and A. Alvarez-Buylla.** 1996. Chain migration of neuronal precursors. Science **271:**978–981.
28. **Luskin, M. B.** 1993. Restricted proliferation and migration of postnatally generated neurons derived from the forebrain subventricular zone. Neuron **11:**173–189.
29. **Margolis, G., and L. Kilham.** 1970. Parvovirus infections, vascular endothelium, and hemorrhagic encephalopathy. Lab. Invest. **22:**478–488.
30. **Margolis, G., L. Kilham, and R. H. Johnson.** 1971. The parvoviruses and replicating cells: insights into the pathogenesis of cerebellar hypoplasia. Prog. Neuropathol. **1:**168–201.
31. **McKisic, M. D., D. W. Lancki, G. Otto, P. Padrid, S. Snook, D. C. Cronin II, P. D. Lohmar, T. Wong, and F. W. Fitch.** 1993. Identification and propagation of a putative immunosuppressive orphan parvovirus in cloned T cells. J. Immunol. **150:**419–428.
32. **McMaster, G. K., P. Beard, H. D. Engers, and B. Hirt.** 1981. Characterization of an immunosuppressive parvovirus related to the minute virus of mice. J. Virol. **38:**317–326.
33. **Miller, R. A., D. C. Ward, and F. H. Ruddle.** 1977. Embryonal carcinoma cells (and their somatic cell hybrids) are resistant to infection by the murine parvovirus MVM, which does infect other teratocarcinoma-derived cell lines. J. Cell Physiol. **91:**393–402.
34. **Miyachi, K., M. J. Fritzler, and E. M. Tan.** 1978. Autoantibody to a nuclear antigen in proliferating cells. J. Immunol. **121:**2228–2234.
35. **Rakic, P., R. S. Cameron, and H. Komuro.** 1994. Recognition, adhesion, transmembrane signaling and cell motility in guided neuronal migration. Curr. Opin. Neurobiol. **4:**63–69.
36. **Rakic, P., and R. L. Sidman.** 1973. Weaver mutant mouse cerebellum: defective neuronal migration secondary to abnormality of Bergmann glia. Proc. Natl. Acad. Sci. USA **70:**240–244.
37. **Ramírez, J. C., A. Fairén, A. Ramírez, E. Lombardo, and J. M. Almendral.** Unpublished data.
38. **Ramírez, J. C., J. A. Santarén, and J. M. Almendral.** 1995. Transcriptional inhibition of the parvovirus minute virus of mice by constitutive expression of an antisense RNA targeted against the NS-1 transactivator protein. Virology **206:**57–68.
39. **Ramón y Cajal, S.** 1960. Studies on vertebrate neurogenesis, p. 253–301. (L. Guth, translator). Charles Thomas, Springfield, Ill.
40. **Ramón y Cajal, S.** 1966. Recollections of my life, p. 370–373 E. H. Craigie, translator). MIT Press, Cambridge, Mass.
41. **Santarén, J. F., J. C. Ramírez, and J. M. Almendral.** 1993. Protein species of the parvovirus minute virus of mice strain MVMp: involvement of phosphorylated VP-2 subtypes in viral morphogenesis. J. Virol. **67:**5126–5138.
42. **Segovia, J. C., J. A. Bueren, and J. M. Almendral.** 1995. Myeloid depression follows infection of susceptible newborn mice with the parvovirus minute virus of mice (strain i). J. Virol. **69:**3229–3232.
43. **Segovia, J. C., A. Real, J. A. Bueren, and J. M. Almendral.** 1991. *In vitro* myelosuppressive effects of the parvovirus minute virus of Mice (MVMi) on hematopoietic stem and committed progenitor cells. Blood **77:**980–988.
44. **Sidman, R. L., M. C. Green, and S. H. Appel.** 1965. Catalog of the neurological mutants of the mouse, p. 66–67. Harvard University Press, Cambridge, Mass.
45. **Siegl, G.** 1988. Patterns of parvovirus disease in animals, p. 43–68. *In* J. R. Pattison (ed.), Parvoviruses and human disease. CRC Press, Boca Raton, Fla.
46. **Siegl, G., R. C. Bates, K. I. Berns, B. J. Carter, D. C. Kelly, E. Kurstak, and P. Tattersall.** 1985. Characteristics and taxonomy of Parvoviridae. Intervirology **23:**61–73.
47. **Spalholz, B. A., and P. Tattersall.** 1983. Interaction of minute virus of mice with differentiated cells: strain-dependent cell specificity is mediated by intracellular factors. J. Virol. **46:**937–943.
48. **Studdert, M. J.** 1990. Tissue tropism of parvoviruses, p. 3–27. *In* P. Tijssen (ed.), Handbook of parvoviruses, vol. II. CRC Press, Boca Raton, Fla.
49. **Tattersall, P.** 1972. Replication of parvovirus minute virus of mice. Dependence of virus multiplication and plaque formation on cell growth. J. Virol. **10:**586–590.
50. **Tattersall, P., and E. M. Gardiner.** 1990. Autonomous parvovirus host-cell interactions, p. 111–121. *In* P. Tjissen (ed.), Handbook of parvoviruses, vol. 1. CRC Press, Boca Raton, Fla.
51. **Tennant, R. W., K. R. Laymant, and R. E. Hand, Jr.** 1969. Effect of cell physiological state on infection by rat virus. J. Virol. **4:**872–878.
52. **Toolan, H. W.** 1990. The rodent parvoviruses, p. 159–176. *In* P. Tjissen (ed.), Handbook of parvoviruses, vol. 1. CRC Press, Boca Raton, Fla.
53. **Török, T. J.** 1992. Parvovirus B19 and human disease. Adv. Intern. Med. **37:**431–455.
54. **Török, T. J., I. Andrews, J. A. Conry, S. Morgello, A. B. MacDonald, J. R. Cafaro, K. Raab, W. A. Bower, E. L. Durigon, S. R. Zaki, and L. J. Anderson.** 1993. Congenital central nervous system disease following intrauterine parvovirus B19 infection. abstr. 7-5. *In* Abstracts of the 5th Parvovirus Workshop, Crystal River, Fla.
55. **Young, N. S.** 1993. B19 parvovirus, p. 75–117. *In* N. S. Young. (ed.), Viruses and bone marrow. Marcel Dekker, New York.
56. **Zheng, C., N. Heintz, and M. E. Hatten.** 1996. CNS gene encoding astrotactin, which supports neuronal migration along glial fibers. Science **272:**417–419.